

Statistical distributions of field-aligned electron events in the near-equatorial magnetosphere observed by the Low Energy Plasma Analyzer on CRRES

G. A. Abel,¹ A. N. Fazakerley, and A. D. Johnstone²

Mullard Space Science Laboratory, University College London, Holmbury St. Mary, Dorking, Surrey, UK

Received 27 August 2001; revised 26 April 2002; accepted 22 August 2002; published 22 November 2002.

[1] Low energy (≤ 100 eV–10 keV) field-aligned electrons are often observed by the Low Energy Plasma Analyzer (LEPA) on the CRRES satellite. These electrons usually occur in bursts of <10 min duration and are mostly bidirectional, though opposing fluxes are not always equal. The events can be seen from L -values of 5 outward (to at least $L = 7$) and from 0800 magnetic local time (MLT) through midnight to 1400 MLT. Larger numbers of events were seen at the outer edge of CRRES' coverage and in the evening and early morning sectors, when the apogee of CRRES was at higher latitudes. The bursts normally occur within 20 min of substorm onset. High-latitude, low-altitude spacecraft often observe upgoing field-aligned electron beams. We suggest that these are the source of the field-aligned electron beams seen by CRRES near the equator. *INDEX TERMS:* 2716

Magnetospheric Physics: Energetic particles, precipitating; 2730 Magnetospheric Physics: Magnetosphere—inner; 2788 Magnetospheric Physics: Storms and substorms; 2736 Magnetospheric Physics: Magnetosphere/ionosphere interactions; *KEYWORDS:* substorms, field-aligned electron distributions, inner magnetosphere, bidirectional electrons

Citation: Abel, G. A., A. N. Fazakerley, and A. D. Johnstone, Statistical distributions of field-aligned electron events in the near-equatorial magnetosphere observed by the Low Energy Plasma Analyzer on CRRES, *J. Geophys. Res.*, 107(A11), 1393, doi:10.1029/2001JA005073, 2002.

1. Introduction

[2] The first observations of field-aligned electron distributions in the near equatorial regions of the magnetosphere at energies <100 keV were reported by *McIlwain* [1975] using the ATS-6 satellite. These electrons were identified as auroral in origin. Earlier spacecraft instrumentation either lacked the angular resolution needed to distinguish field-aligned distributions or did not observe the relevant pitch angles.

[3] Field-aligned electrons have also been reported in the equatorial regions of the magnetosphere by workers using data from the ATS-6 spacecraft [*Parks et al.*, 1977; *Lin et al.*, 1979; *Moore and Arnoldy*, 1982], the GEOS-1 [*Borg et al.*, 1978] and GEOS-2 spacecraft [*Kremser et al.*, 1988], and also the SCATHA (P78-2) satellite [*Richardson et al.*, 1981; *Arnoldy*, 1986]. However, the most complete observations reported to date of counterstreaming electrons in the equatorial region have been made with the AMPTE/CCE satellite [*Klumpar et al.*, 1988; *Klumpar*, 1993]. *Klumpar* [1993] made a statistical survey of counterstreaming electrons in terms of an anisotropy index (see section 6.1). Between 2100 and 0200 magnetic local time (MLT), for

radial distances of $8.75 \pm 0.25 R_E$, occurrence probabilities of counterstreaming electrons were measured to be >40%.

[4] There have also been many observations of field-aligned electron beams made at high latitudes (at altitudes between 1400 km and $\sim 2 R_E$) with a number of spacecraft, S3-3 [*Sharp et al.*, 1980; *Collin et al.*, 1982], ISIS-2 [*Johnstone and Winningham*, 1982; *Klumpar and Heikkila*, 1982], DE-1 [*Lin et al.*, 1982; *Burch et al.*, 1983], VIKING [*Lundin et al.*, 1987; *Hultqvist and Lundin*, 1988; *Hultqvist et al.*, 1988], and Freja [*Boehm et al.*, 1995], and more recently by the FAST satellite [*Carlson et al.*, 1998]. These electron beam observations have been shown to be associated with electrostatic shock structures and field-aligned currents (FACs).

[5] Bidirectional field-aligned electron distributions have also been seen at similar energies in the geomagnetic tail with spacecraft including IMP 6 [*Hada et al.*, 1981], ISEE 1 [*Fairfield and Scudder*, 1985], ISEE 3 [*Baker et al.*, 1986, 1987], GEOTAIL [*Baker et al.*, 1997] and Cassini [*Abel et al.*, 2001]. *Fairfield and Scudder* [1985] suggested that these electrons occupy open lobe field lines and have their source in the solar wind unlike the electron beams presented here, most or all of which occupy closed field lines.

[6] Preliminary studies of the Field-Aligned electron Events (FAEs) observed by CRRES have been presented by *Johnstone et al.* [1994] who suggested that there were three types of FAE. The three types of event are discussed in section 3. By studying detailed energy pitch angle distribu-

¹Now at British Antarctic Survey, Natural Environment Research Council, Cambridge, UK.

²Deceased 28 May 1999.

tions, *Abel et al.* [2002] have shown that during FAEs electrons are scattered out of the field-aligned beam to 90° while simultaneously being accelerated to energies around 10 keV.

[7] In this paper we present the statistical distribution of FAE lifetimes, the spatial distribution of FAEs, and the temporal association with substorms as measured with CRRES. We then go on to discuss these results in the context of the AMPTE/CCE observations made by *Klumpar* [1993] and the low-altitude FAST observations made by *Carlson et al.* [1998] in section 7.

2. Instrumentation

[8] The Combined Release and Radiation Effects Satellite (CRRES) was launched on 25 July 1990 and continued in operation until October 1991, when the spacecraft suffered a fatal power subsystem failure. CRRES was launched into a $350 \times 33,584$ km orbit with an inclination of 18.1° and period of 9 hours and 52 min. The spacecraft was oriented such that its spin axis lay in the ecliptic and pointed 12° ahead of the Sun's apparent motion. In June 1991 the apogee was raised by 1450 km (increasing the orbital period to 10 hours 17 min). The spin period of the spacecraft was 30 s. Further details of the satellite and orbit are given by *Johnson and Ball* [1992].

[9] The survey presented here uses data from the electron sensor of the Low Energy Plasma Analyzer (LEPA). LEPA consists of two triquadrilateral electrostatic analyzers, one configured for electrons and the other for ions. The analyzers are mounted such that the $120^\circ \times 5^\circ$ fan field of view covers angles 30° to 150° with respect to the spacecraft spin axis. This 120° field of view was split into 15 equal anodes, each covering $8^\circ \times 5^\circ$ FOV, and various telemetry modes were utilized so that different portions of the collected data (defined using onboard magnetic field measurements) could be returned. Full details of the LEPA and its operating modes are given by *Hardy et al.* [1993].

3. CRRES/LEPA Observations of FAEs

[10] The LEPA on CRRES is an ideal instrument for finding and studying FAEs as (1) the operational energy range covers that in which FAEs have previously been observed, (2) 180° of pitch angle can be seen at nearly all times, (3) the pitch angle and energy resolution is sufficient to reveal the details in the distribution, and (4) the orbit takes CRRES across a large range of L -shells extending just beyond $L = 8$.

[11] Figure 1 shows examples of two CRRES orbits where FAEs are observed. The figure shows data from the LEPA electron sensor for two orbits, Figure 1a from 23/03/91 and Figure 1b from 31/05/91. In each plot the top panel shows the electron flux measured perpendicular to the field and the lower two show the electron flux in the parallel and antiparallel directions. A clear example of an FAE is seen in Figure 1a. At 1128 the flux observed in all directions increases from a level below the sensitivity of the instrument simultaneously across all energy levels. Between 0.2 and 2 keV the flux levels in the field-aligned directions are greater than that in the perpendicular direction indicating a

field-aligned distribution. At higher energies the flux is strongest in the perpendicular direction. The field-aligned distribution is observed for 6 min after which the fluxes are highest in the perpendicular direction across all energies, decreasing slowly over 5 hours. It is the appearance of these field-aligned fluxes which we term an event. Figure 1b contains a number of FAEs. At 0720 CRRES encounters high fluxes of electrons, however in this example the fluxes are tend to increase over the next few hours, as opposed to the decrease seen in Figure 1a. Between 0820 and 0855 electron fluxes at all levels fall below the sensitivity of the sensors, with the exception of the 5 minute FAE starting at 0834. A number of FAEs are seen throughout this orbit at 0723, 0735, 0748, 0754, 0802, 0808, 0913, 1026, 1058, 1106, and 1111.

[12] LEPA often observes such enhancements in the field-aligned electron fluxes at low energies (<0.1 – 1 keV), simultaneous with increased electron fluxes seen at higher energies across all pitch angles, generally with minima in the field-aligned directions. However, the enhanced field-aligned electron fluxes are not always confined to low energies and have sometimes been seen across the entire energy range observed by LEPA. The electron beams are normally around 15° wide and are not confined to the loss cone, though often it is within the loss cone that the greatest fluxes are seen. The events are generally short-lived with durations typically less than 10 min. Our survey of the LEPA data, covering the entire lifetime of CRRES, found 532 events. Further examples of FAEs are given by *Johnstone et al.*'s [1994] Figure 1 and *Maynard et al.*'s [1996] Plates 4, 5, and 6.

[13] The observed characteristics and context of the events were discussed previously by *Johnstone et al.* [1994] in terms of three types of event. "Substorm" events are seen associated with increases in the overall electron distributions which looked like substorm particle injections or during long lasting injection events. Example of FAEs of the "substorm" type are given by *Johnstone et al.*'s [1994] Figure 1 and *Maynard et al.*'s [1996] Plates 5, and 6. "Sharp onset" events occur when the intensity of electrons increased significantly (often from below the sensitivity of the instrument) across a large energy range. FAEs of the "sharp onset" type are seen within a few minutes of this increase. The events shown in Figure 1a of this paper and *Maynard et al.*'s [1996] Plate 6 show "sharp onset" events. "Sharp onsets" are predominantly seen between 1800 and 2400 MLT. The MLT location and the fact that a sharp onset followed by a slow decay was always seen prompted the suggestion that these events were possibly associated with the westward traveling surge. "Dropout" events were seen when the fluxes of electrons dropped below the LEPA sensitivity for a few minutes. The FAEs were often, though not always, seen at the edges of these flux dropouts. The FAE at 0834 in Figure 1b shows a clear example of an event of the dropout type.

[14] The descriptions of the three types of FAE by *Johnstone et al.* [1994] were based on the appearance of the background plasma populations rather than the field-aligned populations themselves. In fact it is noted that many events share properties of more than one type. For example most "dropout" events are seen within substorm-

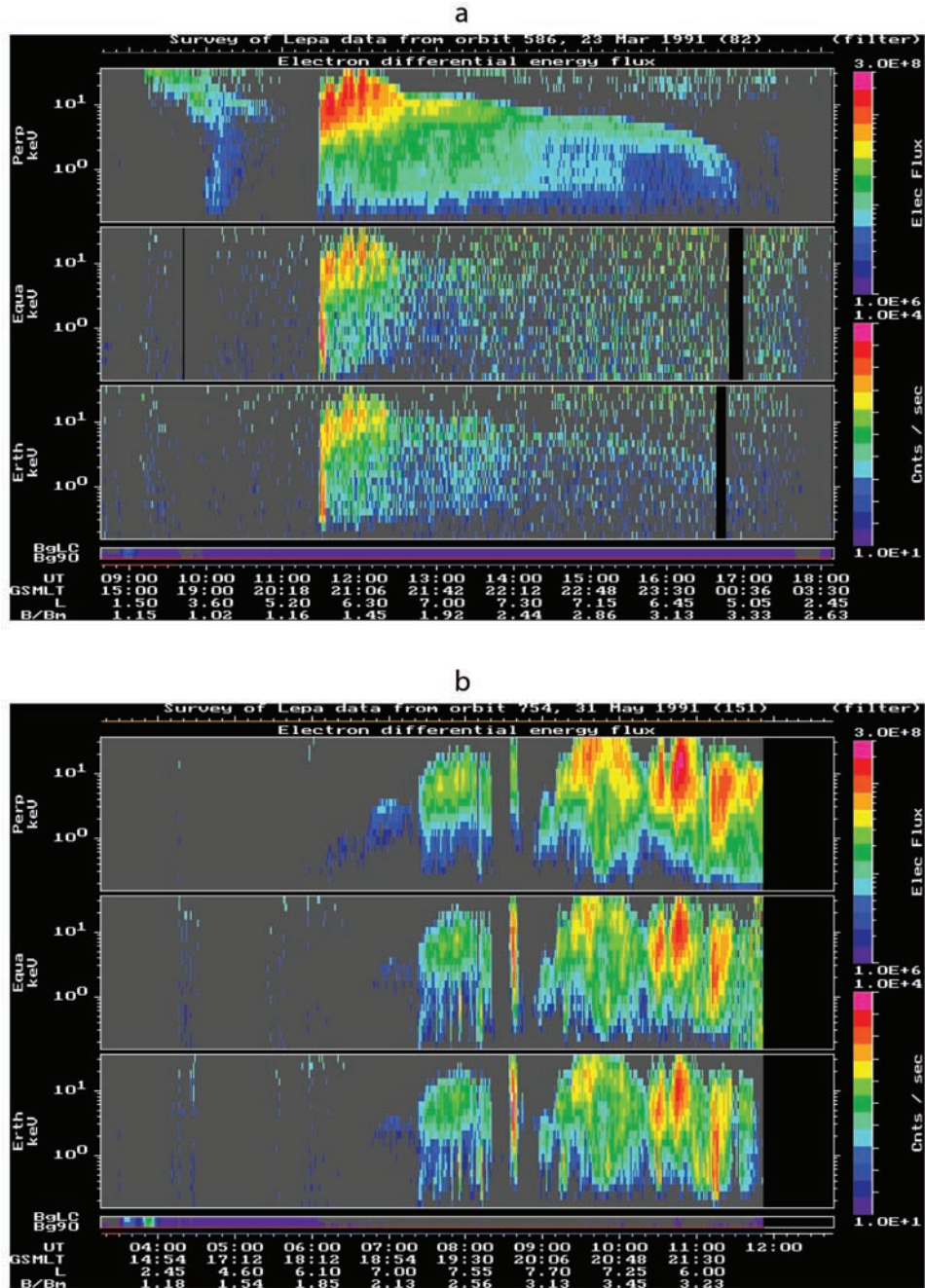


Figure 1. Examples of FAEs. Each panel is an energy time spectrogram with the flux of electrons indicated by the color scale marked Elec Flux. The top panel shows the flux of electrons measured traveling perpendicular to the magnetic field. The lower two panels show the flux of electrons traveling along the field from the equator (middle panel) and from the Earth (lower panel).

like injected electrons though they tend to be seen on higher L-shells than the “substorm” events. Detailed investigation of pitch angle distributions (examples of which are given by *Abel et al.* [2002]) show no difference between the types of events, and in this paper we do not discriminate between the different types of FAE described by *Johnstone et al.* [1994]. The events were selected by studying survey plots of the type presented in Figure 1. They were identified by eye when intense ($>10^7$) fluxes in either of the field-aligned directions were seen to clearly

exceed (by a factor of ~ 3) those in the perpendicular direction.

4. Distribution of FAE Lifetimes

[15] Figure 2 shows the distribution of the observed durations of FAEs. The durations range from 1 to 48 min, but 92% of events lasted for 10 min or less. The modal duration of FAEs is 3 min, while the mean is ~ 5 min.

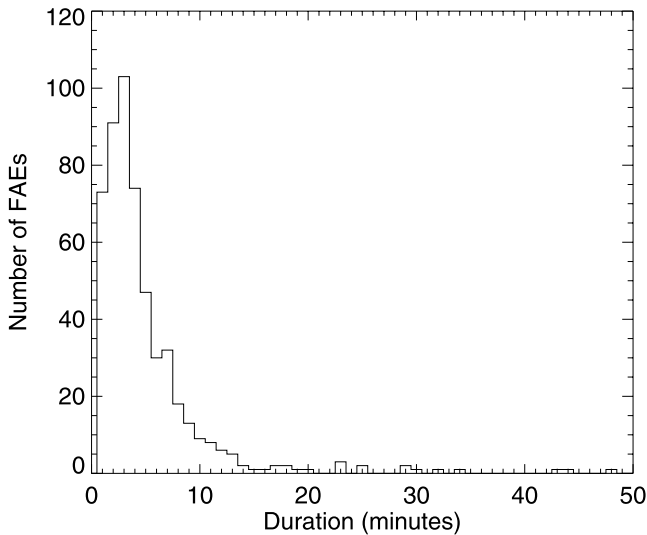


Figure 2. A histogram showing the distribution of durations of 532 FAEs observed by LEPA onboard the CRRES satellite throughout its lifetime.

[16] The colored distribution in Figure 3 shows the distribution of FAE durations against the radial distance of observation site from Earth. Note that as we will discuss the durations in relation to the spacecraft velocity, only events occurring prior to the orbit raising maneuvers in June 1991 (361 of a possible 532) have been used in this figure so as to avoid confusing data collected before and after the change in orbital parameters. We see a trend of increasing durations with increasing orbital radius. The way in which the events vary may be able to provide some indication of the structure of an FAE.

[17] If it were the case that an FAE corresponded to the spacecraft passing through a relatively long-lived structure, then the lifetime of an event would depend on the spacecraft velocity and the shape and dimensions of the structure. We would expect to see a general trend in which shorter events coincide with increasing spacecraft speed and thus decreasing distance from the Earth (as seen in Figure 3). The speed v of a satellite in orbit around the Earth is described by

$$v = \left(GM_E \left(\frac{2}{r} - \frac{1}{a} \right) \right)^{\frac{1}{2}}, \quad (1)$$

where G is the gravitational constant, M_E is the mass of the Earth, r is the distance from the Earth, and a is the semimajor axis of the ellipse describing the satellite's orbital path. If the structures giving rise to the FAEs all had the same linear size measured along the spacecraft track, then by approximating the spacecraft track through the structure to a straight line (which we can do because the spacecraft's velocity remains approximately constant over the few minute duration of the event), the observed lifetime of an event would be proportional to $1/v$ and thus vary with r . If CRRES were to cross a number of structures of varied sizes the distribution of FAE durations with respect to the radial distance of the observation site from Earth will follow curves proportional to $1/v$, with different curves corresponding to structures of different sizes along the spacecraft

trajectory. The red lines marked on Figure 3 are proportional to $1/v$ and clearly do not follow contours of the distribution.

[18] The above argument assumes that the along track dimensions of the structures seen as FAEs are independent of the direction of spacecraft travel. Instead, it is reasonable to expect that they might be organized by the geomagnetic field and thus might have different dimensions in the radial and azimuthal directions, in which case, the duration of an observation of a structure will depend on the direction the spacecraft travel and the form of the structure (see Figure 4). The green curves in Figure 3 are proportional to $1/(v \sin \phi)$, where ϕ is the angle between the satellite's velocity vector and the radial direction. We expect these curves to show how observed durations would vary with r if CRRES crosses a radially extended structures of limited azimuthal extent (Figure 4b). On the other hand, CRRES crossing structures which have limited radial extent, but extended azimuthally (Figure 4c) would result in durations which vary with $1/(v \cos \phi)$, as illustrated by the blue curves shown in Figure 3. The angle ϕ is defined by

$$\sin \phi = \left(\frac{a^2(1 - e^2)}{r(2a - r)} \right)^{\frac{1}{2}}, \quad (2)$$

where e is the eccentricity of the ellipse describing the satellite's orbital path.

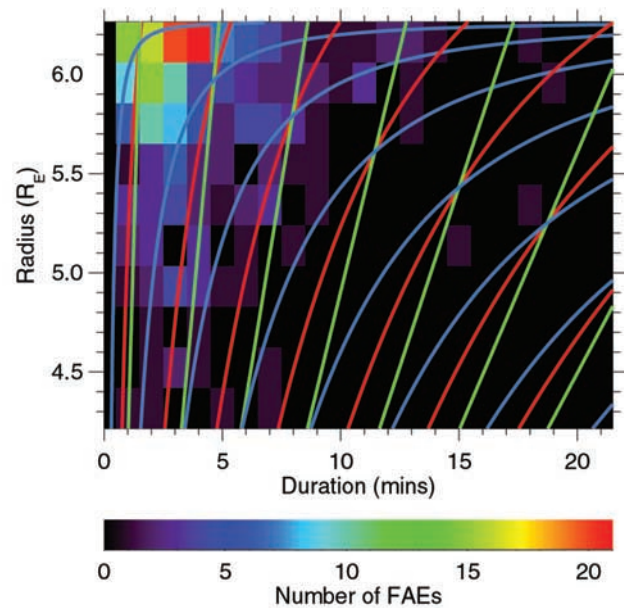


Figure 3. The distribution of durations of FAEs (prior to the orbit raising manoeuvres) against radial distance of the observation site from Earth. The number of events per $0.2 R_E \times 1$ minute bin are represented by the color scale at the bottom of the plot. The red lines represent the expected variation of duration if CRRES were to be passing through a structure of equal dimensions in all directions. The green lines represent the expected variation of duration if CRRES were to be passing through a radially aligned structure of limited azimuthal extent. The blue lines represent the expected variation of duration if CRRES were to be passing through an azimuthally aligned structure of limited radial extent.

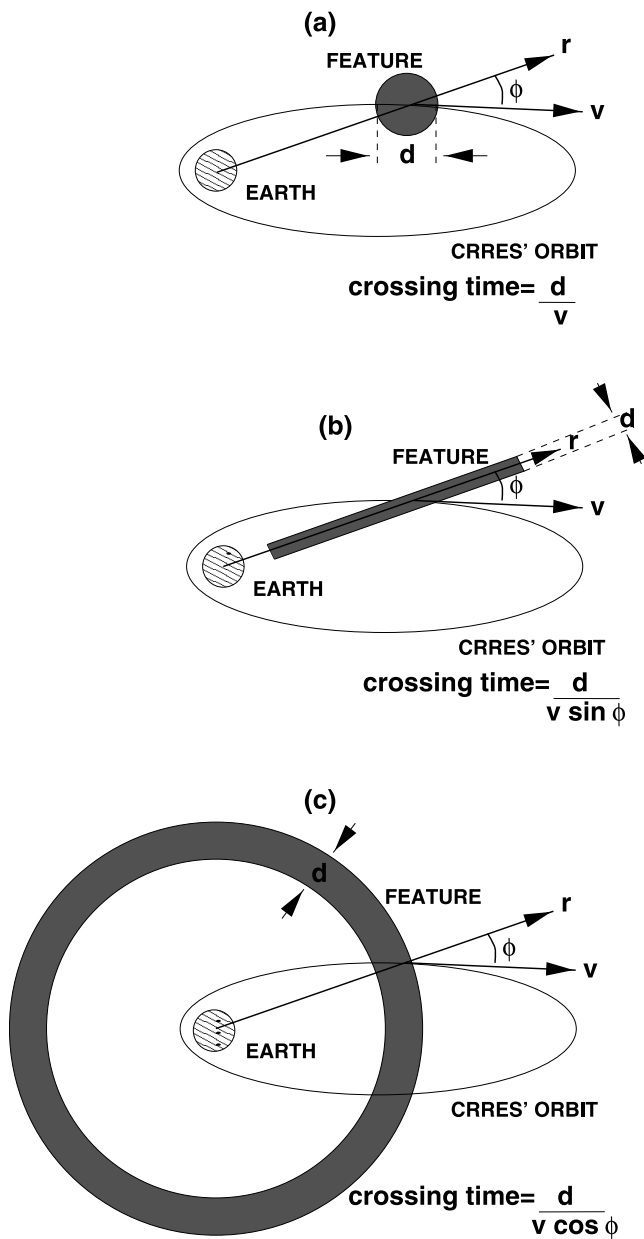


Figure 4. Illustration of the effect of spacecraft motion through relatively long-lived structures of different orientation on the perceived lifetime of an associated event observed by CRRES. (a) A structure with dimensions roughly equal in all directions. An event associated with this structure will have a lifetime which is independent of the direction a spacecraft travels through it. (b) A radially aligned structure of limited azimuthal extent. The lifetime of an event associated with this structure will be dominated by the spacecraft velocity perpendicular to the radial vector and the structure thickness perpendicular to the radial vector. (c) An azimuthally aligned structure of limited radial extent. The lifetime of an event associated with this structure will be dominated by the spacecraft velocity along the radial vector and the structure thickness parallel to the radial vector.

[19] It is clear that the red and green curves in Figure 3 do not follow trend of the distribution of durations shown; however, the blue curves are a better approximation. Assuming FAEs arise as a result of CRRES crossing spatial structures roughly aligned azimuthally with respect to the Earth and having a limited radial extent, we can make some estimate of the radial extent of the events. From the range of blue curves fitting the distribution it appears that the radial dimensions of the structures which would give rise to FAEs are typically between 5×10^4 m and 5×10^5 m.

[20] We propose that the field-aligned electrons are related to the Earth's aurora, which lies in an oval (not strictly azimuthally aligned) around each of the Earth's poles. Given this proposal (and by approximating the Earth's field to a dipole) we estimate the radial extent of the structures crossed by CRRES, when mapped down to the Earth's surface, would correspond to a north-south extent of around 0.3–3 km, which is a good match for the size of typical auroral arc systems [e.g., *Borovsky, 1993*].

[21] This analysis suggests that the observed durations of FAEs can be understood as the consequence of spacecraft motion across a spatially organized structure, which is long-lived relative to the observed FAE duration. It is interesting to note that CRRES often observes a number of events in a sequence (e.g., Figure 1b), which may be explained in terms of CRRES moving through a number of structures at successively greater radial distances, possibly related to a system of nested auroral arcs.

5. Spatial Distribution of FAEs

[22] The spatial distribution of the observed FAEs is shown in Figure 5. The color scale indicates the number of FAEs observed, normalized to the total observation time (in hours) that CRRES spent in each $0.25L \times 30$ minute MLT bin, summed over all latitudes, during its operational lifetime. Bins colored purple indicate regions sampled by CRRES but where no FAEs were observed. Areas colored black were not sampled at all. The L -values have been calculated from the Olsen-Pfitzer 85 field model [*Pfitzer et al., 1988*] for particles mirroring at the spacecraft. Magnetic latitudes between $\pm 20^\circ$ were visited by CRRES though the coverage is biased toward observations south of the equator premidnight and north of the equator postmidnight. In fact it is the combination of the inclination of the orbit and the Earth's dipole tilt which allows us to extend the survey to the highest L -shells.

[23] FAEs are seen throughout CRRES' operational lifetime at most MLTs observed by CRRES but only on L -shells > 4.5 . Despite CRRES spending over 36% of its time inside an L -value of 4.5, only one FAE has been observed in this region. We have found that FAEs are seen only outside of the plasmopause, as determined using observations of the upper hybrid emissions seen in the wave data from the CRRES Plasma Wave Experiment.

[24] As can be seen from Figure 5, beyond $L = 4.5$ occurrence rates vary as a function of L -shell and MLT. Almost no FAEs are seen in the sampled L -range for local times around noon (0800–1500 MLT). Away from noon, FAEs are seen frequently on L -shells > 6 . Peak occurrence rates are found at $L > 7$ at 1700–1930 MLT and 0330–0530

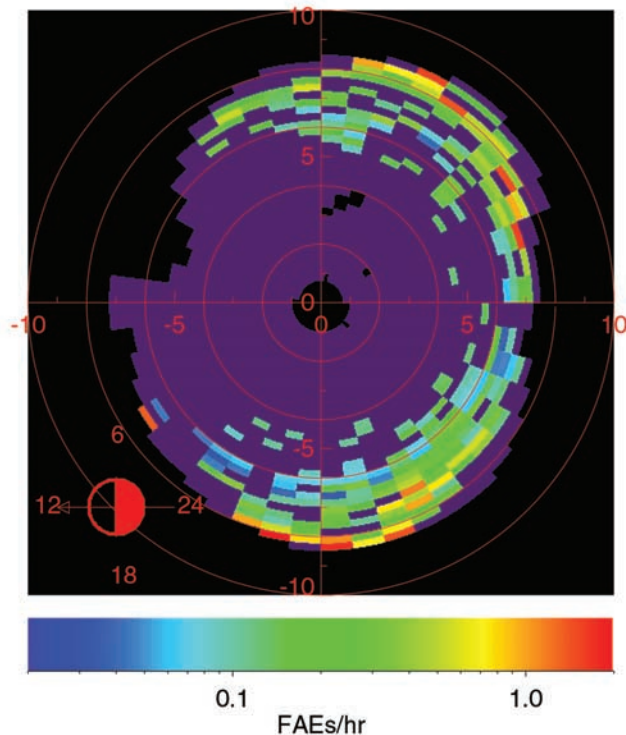


Figure 5. Number of FAEs seen by CRRES normalized to the observation time in each $0.25L \times 30$ min MLT bin summed over all magnetic latitudes. Further explanation of the plot is given in the text.

MLT. The observation rate decreases inward of $L = 7$, reaching zero by $L = 4$. The observation rate is still high at $L = 8$, the outer limit of our observations, and we cannot say whether FAE occurrence rates stay high or fall for $L > 8$. Although coverage around midnight is less on the higher L -shells, there are definitely fewer events in this sector on L -shells for which all MLT are sampled.

6. Association of FAEs With Substorms

[25] *Johnstone et al.* [1994] suggested that one type of FAE (the substorm type) was associated with (not necessarily caused by) magnetospheric substorms, and a second type (the sharp onset type) was possibly related to the westward traveling surge, a feature of the auroral substorm. Here we present further evidence of an association between FAEs and substorms.

[26] A recent study by *Flowers* [1998] has produced a list of 187 substorm onset times for the CRRES epoch, which were identified by looking for dipolarization signatures in the magnetic field data provided by CRRES and the geosynchronous GOES 6 and GOES 7 spacecraft, combined with particle injection signatures in data from the LEPA and EPAS instruments on CRRES, and particle analyzers on a number of LANL spacecraft. The evolution of the particle signatures were used with modeled electron drift times to trace back to the time of onset. A study of intersubstorm intervals by *Borovsky et al.* [1993] found, by monitoring particle injection events on three geosynchronous satellites, that the mean rate of substorm occurrence was 4.2 per day.

This suggests that the *Flowers* [1998] list accounts for around only 10% of substorms that occurred over the 15 month lifetime of CRRES. Some of our FAEs may therefore occur at a time when a substorm occurred that was not included on the *Flowers* [1998] list. Note that the reason that 90% of substorms were not included in the *Flowers* [1998] study was that the study concentrated on clear and definite substorm signatures and employed very stringent selection criteria.

[27] For 95 of the substorms on the list (over half) one or more FAEs are seen in the CRRES LEPA data during the same CRRES orbit. The timings of these FAEs relative to substorm onset time as established by *Flowers* [1998] is shown in Figure 3. The *Flowers* [1998] errors in modeling onset times are estimated to be around 10 to 20 min, with the actual substorm onsets more likely to have occurred prior to the estimated list onset times (substorm onset can only be detected once the magnetic field and particle injection signatures have propagated to the location of the observing spacecraft). For this reason we define a time interval (ΔT), which refers to the closest temporal occurrence of an FAE, either prior to or following substorm onset identified by *Flowers* [1998], within a CRRES orbit (defined as perigee to perigee). It may be the case that the FAE in question is connected not to a listed substorm but to either a previous or following unlisted substorm. There are 62 substorms for which an FAE is observed by CRRES within an hour of estimated onset time, and 52 of these occur within 20 min of onset. The distribution shown in Figure 6 has a secondary peak between 1 hr 50 min and 4 hr 30 min. This peak is small and noisy but appears to be significant (of the 33 FAEs not within 1 hour of substorm onset, 23 of them lie within the 2–4 hour ΔT period). *Borovsky et al.* [1993] found that the distribution of substorm repeat times had a broad peak between 2 and 4 hours and that the modal time between substorm onset was 2.75 hours. The substorms

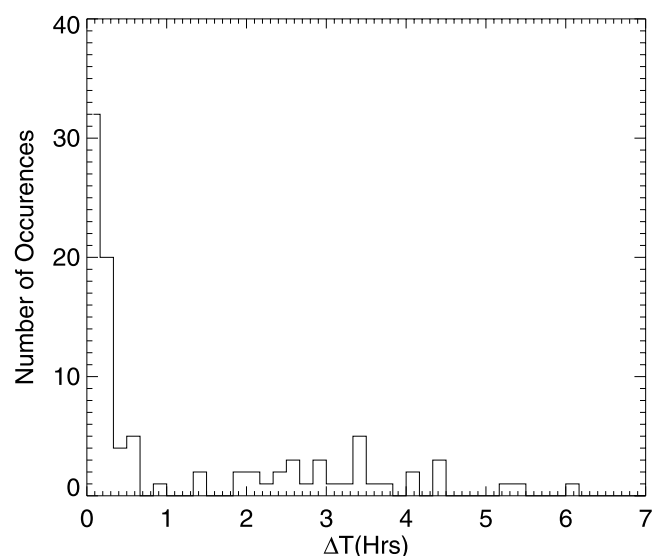


Figure 6. Histogram showing the distribution of times between substorm onset as identified by *Flowers* [1998] and the closest temporal occurrence of an FAE as observed by CRRES.

Table 1. Contingency Table of FAE and Substorm Observation for Each Hour Interval When CRRES Was on L -Shells >5

	FAE Observed	No FAE Observed	Totals
Substorm Observed	45	93	138
No Substorm Observed	240	4822	5062
Totals	285	4915	5200

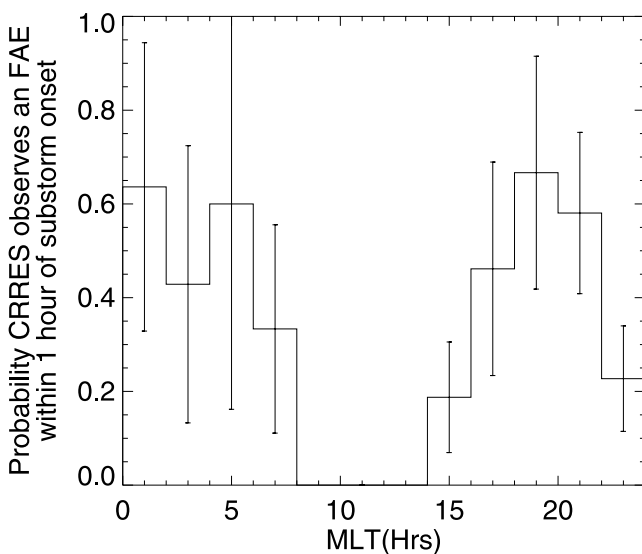
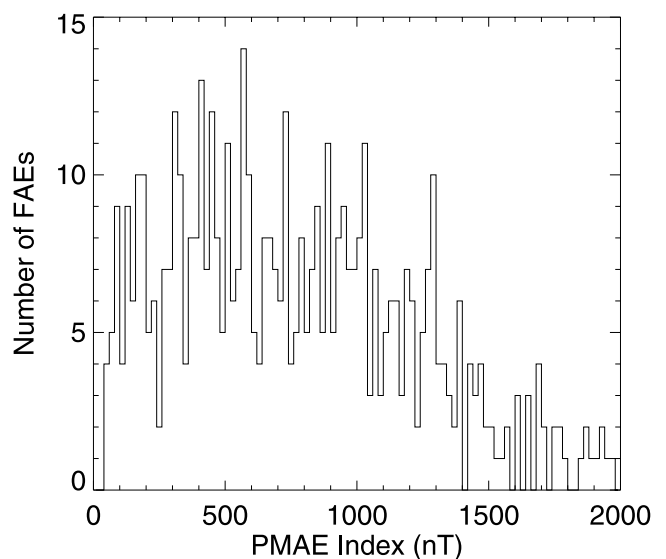
found to be ~ 2.75 hours apart occurred when substorms were taking place in a cyclic fashion. It is not surprising, therefore, that we see a peak in the time between substorm onset and FAE observation between 2 and 4 hours. This peak is likely to correspond to FAEs related to substorm onsets either prior to or following one determined by *Flowers* [1998] but not identified.

[28] The strength of the possible link between FAEs and substorms can be further investigated using a 2×2 contingency table analysis. We have split the lifetime of CRRES into 1 hour periods, excluding times when CRRES is inside $L = 5$, and flagged each one according to whether or not a substorm is listed in the *Flowers* [1998] list and whether or not we observe an FAE. Table 1 shows the results of this survey. Given the number of hours for which substorms were observed and the number of hours for which FAEs were observed, it is possible to calculate the distribution which would be expected if these events were to occur randomly. A chi-square test was applied to the expected and observed values in Table 1 to produce a χ^2 statistic of 201, which is significant at the 0.001 level, i.e., the probability of this distribution occurring by chance is < 0.001 .

[29] The probability of CRRES observing an FAE within 1 hour of substorm onset during times when CRRES is on L -shells >5 is $51 \pm 6\%$. However, as has been shown, the distribution of the observed FAEs is not uniform over all MLT, and thus it would be expected that the probability of observing FAEs within 1 hour of substorm onset would also

vary with MLT. The distribution of these probabilities (for times when CRRES is on L -shells >5) is shown in Figure 7, with error bars calculated from Poisson statistics. It is worth noting at this point that owing to the fact that CRRES was one of the satellites used to determine this list of substorms, the list favors those where CRRES is in a position to see dipolarization and injection events. In fact, over a third of the substorms on the list occur when CRRES is between 2000 MLT and 2400 MLT. However, none of the substorms were identified with data from CRRES alone, and the use of data from other spacecraft allows the calculations to be extended around all local time.

[30] To conclusively demonstrate that all FAEs are associated with substorms it is necessary to show for each event whether or not a substorm is in progress. Therefore the AE index has been studied for each event. However, the AE index is not an ideal proxy for a substorm as FAEs are often seen within 20 min of substorm onset (as defined by *Flowers* [1998]), a time when the auroral electrojet (and thus the AE index) may not have begun to respond strongly to the substorm (typically the AE index will reach its maximum value 30 min to an hour after substorm onset). In order to see if FAEs are related to substorms, we define the Postevent Maximum AE (PMAE) index as the maximum 1 minute value for the AE index in the hour following the event. Figure 8 shows the distribution of the PMAE index for all FAEs observed by CRRES. The average of the PMAE index is 819 nT, and the majority of FAEs occur when the PMAE index is high (>150 nT), reinforcing the argument that these events are substorm-related. There are however a number of FAEs observed when the PMAE index is low, in fact 35 events (6.5%) are seen when the PMAE index does not go above 150 nT. For comparison the distribution of AE index over the CRRES lifetime is shown in Figure 9 where the peak occurrence is seen below 100 nT. It is possible that the FAEs seen at times of low AE may occur at times when the AE index is a poor measure of activity (i.e., the auroral oval may not be lying near its average position, resulting in weaker magnetic signatures at

**Figure 7.** Histogram showing the probability of CRRES observing an FAE within ± 1 hour of estimated substorm onset time (as calculated by *Flowers* [1998]) as a function of MLT for times when CRRES is on L -shells > 5 .**Figure 8.** Histogram showing the distribution of the PMAE index following FAEs.

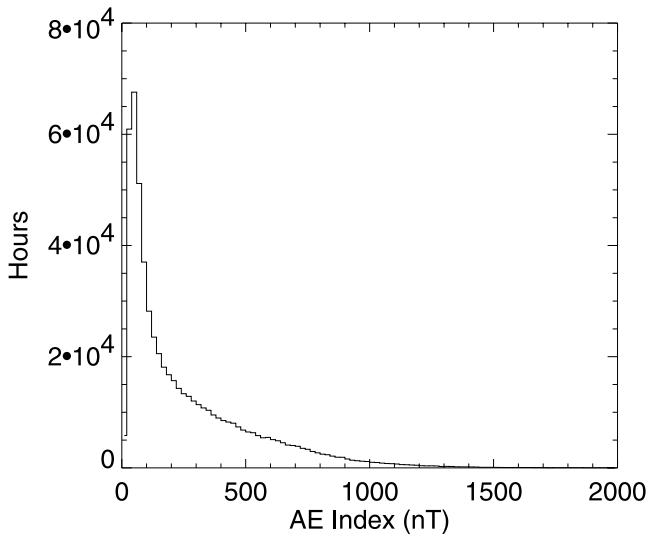


Figure 9. Histogram showing the distribution of the AE index over the CRRES lifetime in terms of the number of hours spent in each 20 nT bin.

the ground magnetometer stations, or the strongest region of the auroral electrojet could lie over Asia where ground station coverage is poor).

7. Discussion

[31] We have found that FAEs are a commonly occurring phenomenon in the magnetosphere possibly related to auroral arcs and apparently occur in conjunction with substorms. In fact, at certain MLTs (0400–0600 MLT and 1800–2000 MLT) the probability of CRRES observing an FAE within an hour of substorm onset is high enough to suggest that FAEs could be present with every substorm and as such may form an integral part of the substorm process. Below we discuss how these observations relate to those made with other spacecraft and the role of FAEs in the magnetospheric system.

7.1. Equatorial Observations

[32] As mentioned in section 1, the most comprehensive observations of equatorial counterstreaming electrons in the existing literature are those detailed by *Klumpar et al.* [1988] and *Klumpar* [1993]. *Klumpar* [1993] using AMPTE/CCE data, suggested the probability of observing counterstreaming electrons was >0.4 (and in some parts of the magnetosphere >0.5). If the observed counterstreaming electrons are the same phenomena as the FAEs described in this paper, then the observations of *Klumpar* [1993] seem inconsistent with our suggestion that the majority of FAEs are related to substorm onset (i.e., substorms are not occurring 40–50% of the time). Their occurrence probabilities are also inconsistent with our result that the peak occurrence rate is 2 FAEs per hour (with a mean duration of 5 min).

[33] Qualitative similarities do exist between the distributions of counterstreaming electrons in the AMPTE/CCE survey and of FAEs in the CRRES survey presented here. First, in both surveys the distribution of FAEs increases with radial distance, with few events seen inside $L = 6$. Second, a minimum at midnight exists in both distributions. In the

AMPTE/CCE survey the midnight minimum is not as wide as that seen in the CRRES data, however, the agreement is generally good. While there are fewer examples of counterstreaming electrons on the dayside compared with the nightside in the AMPTE/CCE data, there are a significant number. However, most of these are seen at radial distances where CRRES has no coverage.

[34] A possible explanation for the discrepancy could lie in the difference between instrumentation used in the two surveys. The LEPA survey presented here has full pitch angle coverage at nearly all times, whereas the AMPTE/CCE Hot Plasma Composition Experiment (HPCE) sensor does not. AMPTE/CCE was spin-stabilized with its spin axis in the equatorial plane. The HPCE included eight 5° full width conical field of view electron sensors, each operating simultaneously at a different fixed energy (0.05–25 keV), mounted with the centers of their FOV perpendicular to the spacecraft spin axis. The data was binned into 6.4 minute averages. Only data collected at those times when the magnetic field direction lay within 10° of the center of the FOV were included in the survey (as only at these times could counterstreaming electrons be detected). If field-aligned electrons are more likely to be seen following substorm onset dipolarisation it may be that they are more likely to be seen during times included in the survey.

[35] In order to further investigate the relationship between the two surveys, we have looked at a subset of LEPA data (at times when $L > 5$, 2200–0200 MLT, $5^\circ < \text{latitude} < 5^\circ$). Owing to the fact that LEPA does not have a sensor with the center of its FOV perpendicular to the spacecraft it has not been possible to mimic the *Klumpar* [1993] directly, so instead we investigate the occurrence probability as a function of the angle between the spin axis and the field direction (θ). We averaged over appropriate energy levels to mimic the HPCE data and calculated an anisotropy measure, as used by *Klumpar* [1993], for each 30 s measurement. The energy bins used were an average of the LEPA energy levels 0, 1 and 3, 4 and 5, 7 and 8, 10 and 11, 13 and 14, 16 and 17, and 19. The anisotropy measure used is simply the ratio of fluxes in the field-aligned direction to fluxes in the perpendicular direction. Figure 10a shows the fraction of measurements where an anisotropy of >1.5 was seen in two or more energy bins, as a function of θ . In fact, by this measure, counterstreaming electrons are less likely toward $\theta = 90^\circ$ (i.e., those times included in the AMPTE/CCE survey). Figure 10b shows the

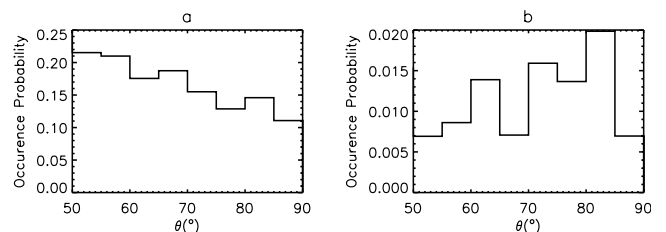


Figure 10. (a) Occurrence probability of exceeding an anisotropy (as described in the text) of 1.5 in two energy bins as a function of θ . (b) Same as Figure 10a but with the added constraint that field-aligned fluxes exceed $3 \times 10^7 \text{ cm}^2 \text{ sr}^{-1} \text{ s}^{-1}$.

results with the added constraint that the parallel fluxes must exceed $3 \times 10^7 \text{ cm}^2 \text{sr}^{-1} \text{s}^{-1}$. In this case we see lower occurrence probabilities than in Figure 10a but with the opposite trend, i.e., counterstreaming electrons are more likely as θ tends to 90° .

[36] The fact that the CRRES study only includes events with intense fluxes appears to be a significant departure from the AMPTE/CCE survey. While the AMPTE/CCE survey no doubt includes the type of event documented here, it will also include lower intensity counterstreaming electrons, which appear to have different occurrence distributions (as indicated by Figure 10). Only by revisiting the AMPTE/CCE data set is it possible to say what the occurrence of intense counterstreaming electrons is at larger L-shells. We should consider the possibility that FAEs themselves are not a substorm related phenomenon, but rather it is the substorm and associated dipolarisation which allows FAEs to be seen in the inner magnetosphere.

7.2. High Latitude Observations

[37] *Carlson et al.* [1998] state that the electron beams seen by FAST are undoubtedly the origin of the highly collimated counterstreaming beams observed deep in the magnetosphere, such as those seen by *Klumpar* [1993]. As we believe that the FAEs seen by CRRES form a subset of the counterstreaming electrons surveyed by *Klumpar* [1993] it is worth comparing them to the upgoing beams seen at high latitudes. The measurements of electron beams made by FAST are by far the highest resolution observations of field-aligned electron beams at high latitudes and we use the example of the auroral oval crossing presented by *Carlson et al.* [1998] as a comparison to the FAEs detailed in this paper. It should be remembered that this is a single example and may not represent typical conditions.

[38] First, the upper energy limit of the beams seen by CRRES and FAST are similar, though the beams seen by FAST often extend to lower energies than those seen by CRRES. However, this apparent difference may be somewhat exaggerated as FAST measured to lower energies than LEPA, and the beams seen by LEPA often extended to the lower limit of LEPA's effective energy coverage (100 eV). The second difference between the beams seen by CRRES and those seen at high latitudes concerns the width of the beam. Most of the reported observations of field-aligned electron beams made at high latitudes suggest beam widths of $\sim 10\text{--}15^\circ$ pitch angle, roughly the same as those seen by CRRES. However, since the magnetic field is weaker at the equator than nearer the poles, we would expect the same beams to be very narrow when seen by CRRES. A certain amount of spread may have been introduced into the CRRES/LEPA data in the construction of the pitch angle energy arrays from the telemetered data products (not discussed here), but this could not account for a beam width of 15° . It is more likely that a very narrow beam would be unstable to wave particle interactions and thus spread in pitch angle en route to CRRES.

[39] The final difference is that the differential energy fluxes seen in the upgoing electron beams in the FAST data are one or two orders of magnitude or more greater than those typically seen by CRRES. In the example presented by *Carlson et al.* [1998] the upgoing differential energy fluxes are typically 10^{10} to $10^{11} \text{ cm}^2 \text{sr}^{-1} \text{s}^{-1}$ compared with

typical values seen in the CRRES events of 10^8 to $10^9 \text{ cm}^2 \text{sr}^{-1} \text{s}^{-1}$ (and our threshold value of $10^7 \text{ cm}^2 \text{sr}^{-1} \text{s}^{-1}$). However, this may be a consequence of the apparent spread in pitch angle. Liouville's theorem states that while moving under adiabatic motion the phase space density of a population of particles remains constant as it moves along a field line. Under these conditions a 15° beam would occupy only very small pitch angles ($\lesssim 0.01^\circ$) when observed near the equator and the phase space density would be the same as is seen at low altitudes. However, the beams are observed over a much larger range of pitch angle and thus occupy a greater amount of velocity space, and hence we would expect to observe lower phase space densities.

[40] Given that the pitch angle width is approximately the same at high latitudes and near the equator we would expect the fluxes to vary proportionally with field strength. The ratio of field strength on a dipole, $L = 6$, field line at $1.6R_E$ (the FAST observations were made at ~ 4000 km) and at the equator is 94. This suggests that the difference in fluxes seen in the FAST data and the CRRES data are consistent with a spreading in pitch angle between high latitudes and the equator. Following this argument, given the beams are seen as counterstreaming near the equator, we would expect to see evidence of them in the downgoing electrons in the FAST data. As it is unlikely that any spreading in pitch angle is a reversible process we would expect to see downgoing electrons covering all pitch angles at similar flux levels as seen in the CRRES events. According to *Carlson et al.*'s [1998] Figure 1, we do indeed see downgoing electrons covering all pitch angles at a flux significantly above the minimum plotted level of $10^7 \text{ cm}^2 \text{sr}^{-1} \text{s}^{-1}$. However, we also see a downgoing field-aligned beam population at higher flux levels than the non-field-aligned electrons but lower than the upgoing beam fluxes. *Carlson et al.* [1998] suggest that the downgoing beam is a result of the upgoing beam electrostatically reflected in the conjugate hemisphere. This is still consistent with our argument if only part of the upgoing beam is scattered in pitch angle. What we observe at CRRES is the pitch angle scattered electrons, with the narrow nonscattered component being smooth out over the 8° sensor FOV. When the electrons are seen as downgoing at FAST, the pitch angle scattered component is spread over all pitch angles, and the nonscattered component is seen as a downgoing beam of lower flux levels than the upgoing beam.

[41] Before the link between the FAEs seen by CRRES and the electron beams seen at lower altitudes can be confirmed, the differences detailed above need to be fully examined. *Lundin et al.* [1987] showed that there were several types of electron beam populations at high latitudes, and the differences between our survey and that of *Klumpar* [1993] show that there are different populations of counterstreaming electrons in the near equatorial magnetosphere. Further investigation into how the different high-latitude beam populations relate to the FAEs seen by CRRES is needed. Nevertheless, it does appear likely that the beams seen by FAST and CRRES are the same phenomenon seen at different locations on a field line.

[42] The conclusion of the *Carlson et al.* [1998] study was that upgoing electron beams were accelerated by diverging electric field, quasi-static potential structures. These structures appear to have similar properties (except

for the reversed polarity) to the converging electrostatic shocks thought to be responsible for accelerating the upgoing ion beams and the downgoing inverted V electrons which produce the auroral light. An optical signature of the diverging shocks when they occur within regions of diffuse aurora is the “black aurora” since precipitation is suppressed [Marklund *et al.*, 1994]. In a more general case they may be considered the “inverse aurora.” This leads to a model of converging and diverging electrostatic shocks forming in the upward and downward current regions, each of which has a number of observational signatures.

[43] In both the upward and downward current regions the beam electrons are carrying significant FAC. Given that the beams seen by FAST and those seen by CRRES appear to be the same phenomenon, the electron beams may be used as a tracer to connect the downward current region into the equatorial regions of the magnetosphere. In this case, FAEs will not map to auroral arcs, but rather “inverse” or “black auroral” arcs within the auroral oval. It is not clear that the counterstreaming electrons seen by CRRES represent a net current flow, and it is beyond the limitations of the instrumentation to demonstrate if there is indeed any net current flow. However, Abel *et al.* [2002] have shown that in most FAEs electrons are seen to be scattered out of the field-aligned beam to 90° while simultaneously being accelerated. This essentially represents a mechanism by which electrons of ionospheric origin can be trapped in the equatorial regions of the magnetosphere resulting in a net flow of electrons (current).

8. Conclusions

[44] We have presented the results of our statistical survey of FAEs seen by CRRES. FAEs are dependent on both position within the magnetosphere and the occurrence of substorms. FAEs are not seen within the plasmasphere, rarely on the dayside, and their occurrence frequency increases with radial distance, with peaks either side of midnight at 0400 MLT and 1930 MLT. Also, FAEs are usually seen within 20 min of substorm onset. We suggest that the source of FAEs is the field-aligned beams seen by FAST and other high-latitude spacecraft, and as such they may play a role as carriers of significant substorm FAC from the auroral acceleration region to the equatorial regions of the magnetosphere. Finally, it should be noted that while FAEs as described here will have been included in the survey of counterstreaming beams presented by Klumpar [1993]. The fact that we have only studied intense beams separates the two studies and may explain the differences in occurrence probabilities and possible association with substorms.

[45] **Acknowledgments.** We are grateful to Nick Flowers for providing the list of substorm onset times. GAA would like to acknowledge a PPARC studentship which funded part of this work.

[46] Arthur Richmond thanks C. W. Carlson and two other reviewers for their assistance in evaluating this paper.

References

- Abel, G. A., A. J. Coates, A. M. Rymer, D. R. Linder, M. F. Thomsen, D. T. Young, and M. K. Dougherty, Cassini CAPS observations of bi-directional lobe electrons during the Earth fly-by, 18th August 1999, *J. Geophys. Res.*, *106*, 30,199–30,208, 2001.
- Abel, G. A., A. N. Fazakerley, and A. D. Johnstone, The simultaneous acceleration and pitch angle scattering of field-aligned electrons observed by the LEPA on CRRES, *J. Geophys. Res.*, *107*, XXXX, doi:10.1029/2001JA005090, in press, 2002.
- Arnoldy, R. L., Fine structure and pitch angle dependence of synchronous orbit electron injections, *J. Geophys. Res.*, *91*, 13,411–13,421, 1986.
- Baker, D. N., S. J. Bame, W. C. Feldman, J. T. Gosling, R. D. Zwickl, J. A. Slavin, and E. J. Smith, Strong electron bidirectional anisotropies in the distant tail: ISEE 3 observations of polar rain, *J. Geophys. Res.*, *91*, 5637–5662, 1986.
- Baker, D. N., S. J. Bame, J. T. Gosling, and M. S. Gussenhoven, Observations of polar rain at low and high altitudes, *J. Geophys. Res.*, *92*, 13,547–13,560, 1987.
- Baker, D. N., A. Nashida, T. Mukai, T. Yamamoto, Y. Saito, Y. Matsuno, S. Kokubun, and T. I. Pulkkinen, Observations of bidirectional electrons in the distant tail lobes: GEOTAIL results, *Geophys. Res. Lett.*, *24*, 959–962, 1997.
- Boehm, M. H., J. Clemmons, J. E. Wahlund, A. Eriksson, L. Eliasson, L. Blomberg, P. Kintner, and H. Hofner, Observations of an upward-directed electron beam with the perpendicular temperature of the cold ionosphere, *J. Geophys. Res.*, *22*, 2103–2106, 1995.
- Borg, H., L. A. Holmgren, B. Hultqvist, F. Cambou, H. Reme, and A. Bahnsen, Some early results of the keV plasma experiment on GEOS-1, *Space Sci. Rev.*, *22*, 511–535, 1978.
- Borovsky, J. B., Auroral arc thicknesses as predicted by various theories, *J. Geophys. Res.*, *98*, 6101–6138, 1993.
- Borovsky, J. B., R. J. Nemzek, and R. D. Belian, The occurrence rate of magnetospheric substorm onsets: Random and periodic substorms, *J. Geophys. Res.*, *98*, 3807–3813, 1993.
- Burch, J. L., P. H. Reiff, and M. Sugiura, Upward electron beams measured by DE-1: A primary source of dayside region-1 Birkeland currents, *Geophys. Res. Lett.*, *10*, 753–756, 1983.
- Carlson, C. W., *et al.*, FAST observations in the downward auroral current region: energetic upgoing electron beams, parallel potential drops, and ion heating, *Geophys. Res. Lett.*, *25*, 2017–2020, 1998.
- Collin, H. L., R. D. Sharp, and E. G. Shelley, The occurrence and characteristics of electron beams over the polar regions, *J. Geophys. Res.*, *87*, 7504–7511, 1982.
- Fairfield, D. H., and J. D. Scudder, Polar rain: solar coronal electrons in the Earth’s magnetosphere, *J. Geophys. Res.*, *90*, 4055–4068, 1985.
- Flowers, N. J., An investigation of substorm particle injections associated with magnetospheric substorms, Ph.D. thesis, Univ. College London, London, September 1998.
- Hada, T., A. Nishida, T. Terasawa, and E. W. Hones Jr., Bi-directional electron pitch angle anisotropy in the plasma sheet, *J. Geophys. Res.*, *86*, 11,211–11,224, 1981.
- Hardy, D. A., D. M. Walton, A. D. Johnstone, M. F. Smith, M. P. Gough, A. Huber, J. Pantazis, and R. Burkhardt, Low Energy Plasma Analyzer, *IEEE Trans. Nucl. Sci.*, *40*, 246–251, 1993.
- Hultqvist, B., and R. Lundin, Parallel electric fields accelerating ions and electrons in the same direction, *Astrophys. Space Sci.*, *144*, 149–154, 1988.
- Hultqvist, B., R. Lundin, K. Stasiewicz, L. Block, P. A. Lindqvist, G. Gustafsson, H. Koskinen, A. Bahnsen, T. A. Potemra, and L. J. Zanetti, Simultaneous observation of upward moving field-aligned energetic electrons and ions on auroral zone field lines, *J. Geophys. Res.*, *86*, 9765–9776, 1988.
- Johnson, M. H., and J. K. Ball, Combined Release and Radiation Effects Satellite (CRRES): Spacecraft and mission, *J. Spacecraft Rockets*, *29*, 556–563, 1992.
- Johnstone, A. D., and J. D. Winningham, Satellite observations of suprathermal electron bursts, *J. Geophys. Res.*, *87*, 2321–2329, 1982.
- Johnstone, A. D., N. J. Flowers, and R. Liu, Observations in the equatorial region of the field-aligned electron and ion distributions in the energy range 100 eV to 5 keV associated with substorm onsets, in *Proceedings of the Second International Conference on Substorms, Fairbanks, Alaska*, Geophys. Inst., Univ. of Alaska, Fairbanks, Alaska, 1994.
- Klumpar, D. M., Statistical distributions of the auroral electron albedo in the magnetosphere, *Auroral Plasma Dynamics, Geophys. Monogr. Ser.*, vol. 80, edited by R. L. Lysak, pp. 163–171, AGU, Washington, D. C., 1993.
- Klumpar, D. M., and W. J. Heikkila, Electrons in the ionospheric source cone: evidence for runaway electrons as carriers of downward birkeland currents, *Geophys. Res. Lett.*, *9*, 873–876, 1982.
- Klumpar, D. M., J. M. Quinn, and E. G. Shelley, Counterstreaming electrons at the magnetic equator near $9 R_E$, *Geophys. Res. Lett.*, *15*, 1295–1298, 1988.
- Kremser, G., A. Korth, S. L. Ullaland, S. Perraut, A. Roux, A. Pedersen, R. Schmidt, and P. Tanskanen, Field-aligned beams of energetic electrons ($16 \text{ keV} \leq E \leq 80 \text{ keV}$) observed at geosynchronous orbit at substorm onsets, *J. Geophys. Res.*, *93*, 14,453–14,464, 1988.

- Lin, C. S., G. K. Parks, S. DeForest, and C. E. McIlwain, Temperature characteristics of electron beams and ambient particles, *J. Geophys. Res.*, *84*, 2651–2654, 1979.
- Lin, C. S., J. L. Burch, J. D. Winningham, J. D. Menietti, and R. A. Hoffman, DE-1 observations of counterstreaming electrons at high altitudes, *Geophys. Res. Lett.*, *9*, 925–928, 1982.
- Lundin, R., L. Eliasson, B. Hultqvist, and K. Stasiewicz, Plasma energization on auroral field lines as observed by the VIKING spacecraft, *Geophys. Res. Lett.*, *14*, 443–446, 1987.
- Marklund, G., L. Blomberg, C.-G. Falthammar, and P.-A. Lindqvist, On intense diverging electric fields associated with black aurora, *Geophys. Res. Lett.*, *21*, 1859–1862, 1994.
- Maynard, N. C., W. J. Burke, E. M. Basinska, G. M. Erickson, W. J. Hughes, H. J. Singer, A. G. Yahnin, D. A. Hardy, and F. S. Mozer, Dynamics of the inner magnetosphere near times of substorm onsets, *J. Geophys. Res.*, *101*, 7705–7736, 1996.
- McIlwain, C. E., Auroral beams near the magnetic equator, in *The Physics of Hot Plasmas in the Magnetosphere*, edited by B. Hultqvist and L. Stenflow, p. 91, Plenum, New York, 1975.
- Moore, T. E., and R. L. Arnoldy, Plasma pitch angle distributions near the substorm injection front, *J. Geophys. Res.*, *87*, 4405–4417, 1982.
- Parks, G. K., C. S. Lin, B. H. Mauk, S. DeForest, and C. E. McIlwain, Characteristics of magnetospheric particle injection deduced from events observed on August 18, 1974, *J. Geophys. Res.*, *82*, 5208–5214, 1977.
- Pfizer, K. A., W. P. Olson, and T. Mogstad, A time dependent source driven magnetospheric field model (abstract), *Eos Trans. AGU*, *69*(426), 1988.
- Richardson, J. D., J. F. Fennel, and D. R. Croley Jr., Observations of field-aligned ion and electron beams from SCATHA (P78-2), *J. Geophys. Res.*, *86*, 10,105–10,110, 1981.
- Sharp, R. D., E. G. Shelley, R. G. Johnson, and A. G. Ghielmetti, Counterstreaming electron beams at altitudes of $\sim 1 R_E$ over the auroral zone, *J. Geophys. Res.*, *85*, 92–100, 1980.

G. A. Abel, British Antarctic Survey, High Cross, Madingley Road, Cambridge CB3 0ET, UK. (gaab@bas.ac.uk)

A. N. Fazakerley, Mullard Space Science Laboratory, University College London, Holmbury St. Mary, Dorking, Surrey, RH5 6NT, UK. (anf@mssl.ucl.ac.uk)